J|A|C|S COMMUNICATIONS

Published on Web 02/06/2009

Oxygen−Oxygen Bond Formation by the Ru-Hbpp Water Oxidation Catalyst Occurs Solely via an Intramolecular Reaction Pathway

Sophie Romain, Fernando Bozoglian, Xavier Sala, and Antoni Llobet*

Institute of Chemical Research of Catalonia (ICIQ), Avinguda Països Catalans 16, E-43007 Tarragona, Spain, and Departament de Química, Universitat Autònoma de Barcelona, Cerdanyola del Vallès, E-08193 Barcelona, Spain

Received October 21, 2008; E-mail: allobet@iciq.es

The oxidation of water to molecular dioxygen is a reaction that takes place in the dark with the photosystem II oxygen-evolving complex (OEC-PSII).[1] It is a very interesting reaction to model from a bioinorganic perspective, since it can give some hints regarding the potential mechanisms that operate in this natural system. On the other hand, it is of tremendous importance from an energetic perspective, since it is recognized to be the bottleneck for the development of commercial light-harvesting devices for the photoproduction of H_2 from water.[2] Water oxidation is a challenging task for a catalyst for two main reasons. One is the strongly uphill thermodynamics for the reaction

$$2H_2O \rightarrow O_2 + 4H^+ + 4e^-$$

for which $E° = 1.23$ V (vs SCE) at pH 0. The other is the high molecular complexity of this reaction from a mechanistic point of view, since two protons and two electrons have to be removed from each water molecule, and furthermore, an oxygen−oxygen bond has to be formed. There are a few complexes characterized at a molecular level that have been described in the literature to be capable of catalytically oxidizing water to molecular dioxygen,[3] and *only* the so-called "blue dimer" $\{cis,cis\text{-}[Ru(bpy)_2(H_2O)]_2(\mu\text{-}O)^{4+}\}$ has been studied mechanistically, with rather controversial results.[4,5] *The two main challenges in the field are actually understanding the reaction mechanism and finding an efficient and rugged catalyst.*

A few years ago, we reported[6] a new water oxidation catalyst, $\{[Ru^{II}(trpy)(H_2O)]_2(\mu\text{-bpp})\}^{3+}$ [Ru-Hbpp; trpy = 2,2′:6′,2″-terpyridine, bpp = 2,6-bis(pyridyl)pyrazolate], that contains a pyrazolate rather than an oxo bridging ligand; its structure is presented in Figure 1. We now report a thorough kinetic analysis combined with ^{18}O labeling experiments that allows us to clearly elucidate the reaction mechanism. Electron-transfer (ET) kinetic experiments were carried out over a temperature range of 10−40° for the four one-electron processes, and the corresponding k_{ETn} ($n = 1-4$) values and activation parameters are presented in Table 1.

The four ET processes were found to be first order with respect to both the catalyst and Ce(IV) under all of the conditions we studied. It is interesting to observe that the rate constant decreases as the oxidation state increases, with the last step being the slowest one. No oxygen evolution is observed until the $Ru^{IV,IV}$ oxidation state is reached, and thus, the values k_{ET1}, k_{ET2}, and k_{ET3} (i.e., up to the III,IV oxidation state) can be calculated independently of the other kinetic processes that finally generate the oxygen−oxygen bond.

After the IV,IV oxidation state is attained, an intermediate species **I** is detected prior to the events that lead to oxygen evolution and formation of the initial Ru^{II} complex (see the bottom panel of Figure 2), as evidenced by the time-resolved UV−vis spectra shown in Figure S1 in the Supporting Information and their mathematical

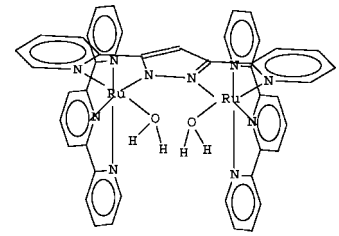

Figure 1. Drawn structure of Ru-Hbpp.

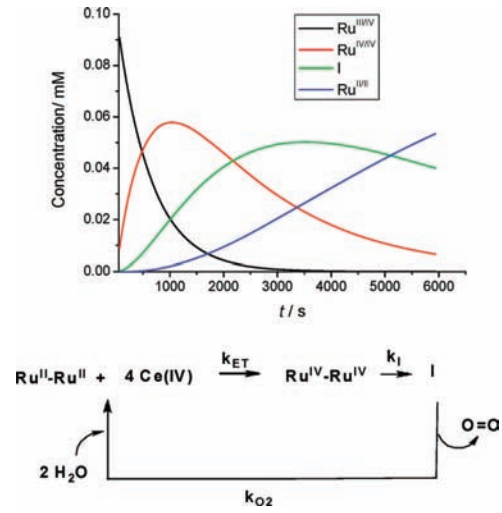

Figure 2. (top) Species distribution diagram for the reaction of 1.0×10^{-4} M Ru-Hbpp solution with 4 equiv of Ce(IV) in 0.1 M CF_3SO_3H at 10.0 °C. Species calculated with three consecutive first order reactions (A → B → C → D). (bottom) Reaction scheme for generation of O_2 upon addition of Ce(IV) to Ru-Hbpp.

treatment with Specfit.[7] The obtained species distribution diagram is shown in the top panel of Figure 2.

These last two processes are first-order, and their rate constant values and activation parameters are also listed in Table 1. As can be observed from these data, these two processes are much slower than the initial ET processes. In order to extract further mechanistic information, oxygen labeling experiments were carried out using $H_2{}^{18}O$ to label the catalyst and also as the solvent. It is known for related polypyridylic Ru^{II}−L (L = Cl, H_2O) chemistry[8] that the rate of L substitution dramatically decreases as the oxidation state of the metal center increases. In our particular case, using the MeCN analogue (Ru−H_2O + MeCN → Ru−MeCN + H_2O) to finally make $\{[Ru^{III}(trpy)(H_2O)](\mu\text{-bpp})[Ru^{III}(trpy)(MeCN)]\}^{5+}$, we found that at the III,III oxidation state, the pseudo-first-order rate constant was 2.05×10^{-5} s^{-1}. This enabled us to perform water oxidation experiments with different degrees of labeling of both the catalyst and the solvent. The experiments were designed so only one metal

10.1021/ja808166d CCC: $40.75

Table 1. Rate Constants Calculated at 10.0 °C and the Corresponding Activation Parameters for Steps in the Reaction of the Ru-Hbpp Catalyst and Ce(IV) in 0.1 M CF_3SO_3H

k	process	k value	$\Delta H^{\ddagger}$ (kJ mol^{-1})	$\Delta S^{\ddagger}$ (J mol^{-1} K^{-1})
		ET Rate Constants k_{ETn} (M^{-1} s^{-1})		
k_{ET1}	$Ru^{II/II} \rightarrow Ru^{II/III}$	$(5.0 \pm 0.3) \times 10^4$	22 ± 1	-84 ± 3
k_{ET2}	$Ru^{II/III} \rightarrow Ru^{III/III}$	$(3.9 \pm 0.1) \times 10^4$	34 ± 2	-45 ± 7
k_{ET3}	$Ru^{III/III} \rightarrow Ru^{III/IV}$	$(3.2 \pm 0.2) \times 10^4$	29 ± 2	-65 ± 5
k_{ET4}	$Ru^{III/IV} \rightarrow Ru^{IV/IV}$	$(5.0 \pm 0.8) \times 10^2$	23 ± 3	-122 ± 10
		Rate Constants for Formation of **I** and O_2 (s^{-1})		
k_I	$Ru^{IV/IV} \rightarrow$ **I**	$(6.1 \pm 0.3) \times 10^{-4}$	53 ± 3	-137 ± 9
k_{O_2}	**I** $\rightarrow Ru^{II/II}$	$(1.4 \pm 0.1) \times 10^{-4}$	85 ± 8	-39 ± 27

Table 2. Relative Isotopic Ratios of Evolved Molecular Oxygen in the First Metal Cycle Using Different Degrees of Labeled Catalyst and Solvent and the Corresponding Calculated Values Assuming Different Reaction Mechanisms[a]

	^{18}O labeling (%)[b]		isotopic ratios				
entry	catalyst	solvent	O_2	exch[c]	nuc[d]	intra[e]	exptl
1	0	12.00	$^{16}O_2$	77.44	88.00	99.52	99.50
2			$^{16}O^{18}O$	21.12	12.00	0.48	0.47
3			$^{18}O_2$	1.44	2×10^{-4}	4×10^{-4}	0.03
4	16.13	11.90	$^{16}O_2$	77.60	74.60	70.34	69.97
5			$^{16}O^{18}O$	21.00	14.50	27.05	27.48
6			$^{18}O_2$	1.40	1.90	2.61	2.55
7	22.73	18.52	$^{16}O_2$	66.39	62.96	59.70	60.20
8			$^{16}O^{18}O$	30.18	32.83	35.13	35.10
9			$^{18}O_2$	3.43	4.21	5.17	4.70

[a] See the Supporting Information for experimental details. [b] These columns indicate the degree of ^{18}O labeling of the catalyst and the solvent. [c] Calculated ratios of isotopic O_2 obtained in the case of a fast exchange ("exch") process with the solvent. [d] Calculated ratios in the case of nucleophilic ("nuc") attack by the solvent on the Ru=O groups. [e] Calculated ratios in the case of intramolecular ("intra") oxygen−oxygen coupling from the Ru=O groups.

Scheme 1. Potential Mechanistic Pathways for the Formation of O_2 Involving the Ru Metal Centers

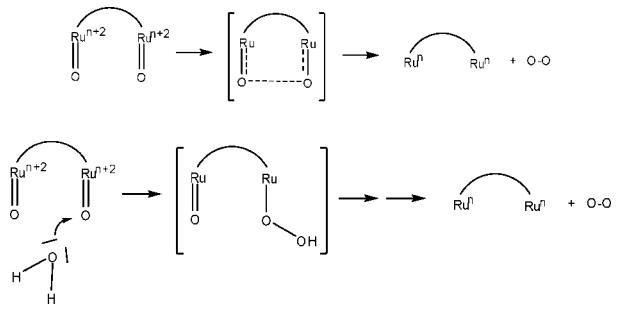

cycle could take place, and the gases formed were analyzed online via mass spectrometry. In Table 2 are listed the results of the labeling experiments using different degrees of labeling of the catalyst and solvent.

The two considered mechanisms termed "intramolecular O−O bond formation" (intra) and "H_2O nucleophilic attack" (nuc)[9] are graphically presented in the top and bottom panels, respectively, of Scheme 1. The present labeling experiments unquestionably demonstrate that the only mechanism operating in our case is the intramolecular one. This is in sharp contrast with a recently published density functional theory study[10] claiming that the mechanism is mainly nucleophilic addition. Our results strongly indicate that this work should be revised.

The results found here are radically different from those observed for the ^{18}O-labeled blue dimer, where the intramolecular pathway is very minor and the most important Ru-based pathway seems to be water nucleophilic addition. In our particular case, however, both the structure and electronic properties of the Ru-Hbpp catalyst are radically different from those of the blue dimer.[6] In the Ru-Hbpp case, the bridging ligand is rigid and the molecule is designed in such a way that two $Ru-OH_2$ moieties are oriented cis to one another. We have multiple evidence of through-space interactions of the two L groups in the II,II oxidation state that supports this concept. Thus, when the highest oxidation state is reached, the oxygen atoms are ready to couple to one another and thus favor the intramolecular mechanism.[11] We are at the moment directing our efforts toward further spectroscopic (EPR, XPS, rR) characterization of the intermediate reaction species **I** that is formed prior to oxygen evolution, which we hypothesize could be a *cis*-η^1:η^1-peroxo-bridged bis[Ru(III)] complex.

The present work constitutes a successful mechanistic study in which the reaction pathway for water oxidation has been characterized kinetically, forming the basis for further development of efficient water oxidation catalysts.

Acknowledgment. Support form SOLAR-H2 (EU 212508), ACS (PRF 46819-AC3), and Consolider Ingenio 2010 (CSD2006-0003) are gratefully acknowledged. X.S. thanks MICINN for a Torres Quevedo contract.

Supporting Information Available: Experimental details and additional kinetic and labeling data. This material is available free of charge via the Internet at http://pubs.acs.org.

References

(1) (a) Yano, J.; Kern, J.; Sauer, K.; Latimer, M. J.; Pushkar, Y.; Biesiadka, J.; Loll, B.; Saenger, W.; Messinger, J.; Zouni, A.; Yachandra, V. K. *Science* **2006**, *314*, 821. (b) Haumann, M.; Liebisch, P.; Müller, C.; Barra, M.; Grabolle, M.; Dau, H. *Science* **2005**, *310*, 1019.
(2) Balzani, V.; Credi, A.; Ventura, M. *ChemSusChem.* **2008**, *1*, 26.
(3) Sala, X.; Rodriguez, M.; Romero, I.; Escriche, L.; Llobet, A. *Angew. Chem., Int. Ed.*, in press.
(4) (a) Binstead, R. A.; Chronister, C. W.; Ni, J.; Hartshorn, C. M.; Meyer, T. J. *J. Am. Chem. Soc.* **2000**, *122*, 8464. (b) Liu, F.; Concepcion, J. J.; Jurss, J. W.; Cardolaccia, T.; Templeton, J. L.; Meyer, T. J. *Inorg. Chem.* **2008**, *47*, 1727.
(5) Yamada, H.; Siems, W. F.; Koike, T.; Hurst, J. K. *J. Am. Chem. Soc.* **2004**, *126*, 9786.
(6) Sens, C.; Romero, I.; Rodríguez, M.; Llobet, A.; Parella, T.; Benet-Buchholz, J. *J. Am. Chem. Soc.* **2004**, *126*, 7798.
(7) Specfit is a trademark of Spectrum Software Associates.
(8) Yamada, H.; Koike, T.; Hurst, J. K. *J. Am. Chem. Soc.* **2001**, *123*, 12775.
(9) Romero, I.; Rodriguez, M.; Sens, C.; Mola, J.; Kollipara, M. R.; Francas, L.; Mas-Marza, L.; Escriche, E.; Llobet, A. *Inorg. Chem.* **2008**, *47*, 1824.
(10) Yang, X.; Baik, M.-H. *J. Am. Chem. Soc.* **2008**, *130*, 16231.
(11) Evidence for this type of mechanism has also been found in the case of dinitrogen formation using a related oxo-bridged dimer. See: Ishitani, O.; Ando, E.; Meyer, T. J. *Inorg. Chem.* **2003**, *42*, 1707.

JA808166D